

SUPPORTING INFORMATION

Synoptic timescale linkage between midlatitude winter troughs Sahara temperature patterns and northern Congo rainfall: A building block of regional climate variability

Neil Ward, Andreas H. Fink, Richard J. Keane, Françoise Guichard,
John H. Marsham, Douglas J. Parker, Christopher M. Taylor

1. Supporting Tables

TABLE S1 Specification regression equation (zero lead) for daily OLR (-W/m²) over the NEC and NWC domains, using predictors Q925 (g/kg), U925 (m/s) and Q600 (g/kg) (domains as defined in Table 2). The results are similar to Table 4 but now models are fit separately in each month November through March. These results confirm that the specification equation for November has similar structure and explanatory power when compared to December-March. Significance p-value (sig) is provided for guidance, without attempt to adjust degrees of freedom for serial correlation. Final column gives the multiple correlation fit of the model (mult corr). (In all regression analyses, the regression model constant a_0 is fitted but not shown).

Pred	Month	Q925			U925			Q600			mult corr
		Coeff	tval	sig	Coeff	tval	sig	Coeff	tval	sig	
NEC	Nov	6.34	10.36	0.000	7.52	13.76	0.000	5.97	9.19	0.000	0.61
	Dec	2.76	8.24	0.000	4.12	7.54	0.000	5.80	9.59	0.000	0.56
	Jan	2.07	6.56	0.000	4.15	6.66	0.000	5.51	8.53	0.000	0.56
	Feb	3.29	9.36	0.000	3.99	6.38	0.000	6.13	7.39	0.000	0.61
	Mar	5.64	12.65	0.000	6.08	10.97	0.000	5.89	8.47	0.000	0.65
NWC	Nov	8.64	9.44	0.000	4.51	6.25	0.000	5.46	8.96	0.000	0.49
	Dec	3.98	8.52	0.000	4.81	7.16	0.000	4.19	7.82	0.000	0.52
	Jan	3.00	6.94	0.000	4.59	5.65	0.000	5.24	8.65	0.000	0.53
	Feb	3.12	5.89	0.000	6.32	6.99	0.000	7.09	8.84	0.000	0.55
	Mar	7.80	11.45	0.000	5.91	7.87	0.000	6.47	9.04	0.000	0.56

TABLE S2 Prediction regression equation (2-day lead) for OLR (-W/m²) over the NEC and NWC domains. Predictor T850 (°C) indices (N45 for NEC and N23 for NWC) and OLR index (EGC, -W/m²) located on Figure 1. The results are similar to Table 5 but now models are fit separately in each month October through April. Results confirm (i) The T850 predictor loses all or most of its predictive power in October and April, illustrating why these months are mostly not considered in this paper, (ii) in December-March, T850 always displays strong explanatory power (very high t-values), (iii) in November, T850 has moderately strong explanatory power, but noticeably weaker than in December-March (and EGC loses skill in November for NWC). Overall, November is considered to partially display the signature synoptic sequence of NE Africa warming leading to increased convection/rainfall. It is noteworthy that EGC is a powerful predictor of both NEC and NWC in April, leading to a moderate multiple correlation (but without the T850 signature, April is considered to have different character compared to December-March in terms of the primary features under consideration in this paper).

Pred	Month	T850			EGC			mult corr
		Coeff	tval	sig	Coeff	tval	sig	
NEC	Oct	-0.16	-0.25	0.803	0.12	4.00	0.000	0.12
	Nov	4.85	10.34	0.000	0.10	3.12	0.002	0.33
	Dec	4.12	13.42	0.000	0.09	2.64	0.008	0.41
	Jan	3.39	12.84	0.000	0.22	6.15	0.000	0.47
	Feb	3.83	13.91	0.000	0.24	7.82	0.000	0.53
	Mar	4.78	16.19	0.000	0.17	6.62	0.000	0.53
	Apr	2.14	4.60	0.000	0.26	9.99	0.000	0.34
NWC	Oct	-2.17	-3.54	0.000	0.02	0.90	0.366	0.11
	Nov	3.85	6.97	0.000	-0.03	-0.84	0.401	0.21
	Dec	4.60	13.68	0.000	0.05	1.41	0.158	0.41
	Jan	3.11	10.54	0.000	0.23	6.34	0.000	0.43
	Feb	3.38	10.49	0.000	0.27	8.32	0.000	0.48
	Mar	4.02	10.30	0.000	0.13	4.55	0.000	0.38
	Apr	0.90	1.61	0.108	0.21	7.59	0.000	0.24

2. Supporting Figures

FIGURE S1 Number of 10-percentile daily values for NEC OLR in (a) November, (b) December, (c) January, (d) February, (e) March. (f)-(j) Same as (a)-(e) but for NWC OLR. Results are for 1982-2016. The 10-percentile threshold is calculated separately for each month (through a simple ranking of values). In red is linear trend and associated significance (p , noted if $p < 0.2$, otherwise listed as n.s., not significant), which are shown to aid visual inspection (trend significance does not account for residual serial correlation, which may increase the p-values shown). This figure (as well as Figures S2 and S3) confirms that results of the compositing are not expected to be dominated by trend features.

FIGURE S2 Same as Figure S1 but using 20-percentile daily values of IMERG rainfall data with results over 2001-2016.

FIGURE S3 Same as Figure S2 but using trough parameter daily values 1982-2016 for (a)-(e) Iberia troughs and (f)-(j) CMed troughs.

FIGURE S4 Same as Figure 3 but using IMERG precipitation to identify the wettest 20% of days 2001-2016.

FIGURE S5 Same as Figure 5 but adding 850-hPa anomaly wind vector composites (with vector calculation and significance inclusion as described in Figure 9 caption).

FIGURE S6 Same as Figure 8 but for 600-hPa specific humidity and wind, and with specific humidity contours at ± 0.2 and 0.6 g/kg . This figure confirms the results in Figure 8 over highland areas such as parts of East Africa where, in Figure 8, results contain some values interpolated to below the surface (850-hPa), but here these are nonetheless shown to be synoptically consistent with the 600-hPa level.

FIGURE S7 Same as Figure 10 but (a) for December (with wind plotted at 5% significance threshold), (b) MCS activity averaged over $0\text{-}28^\circ\text{E}$.

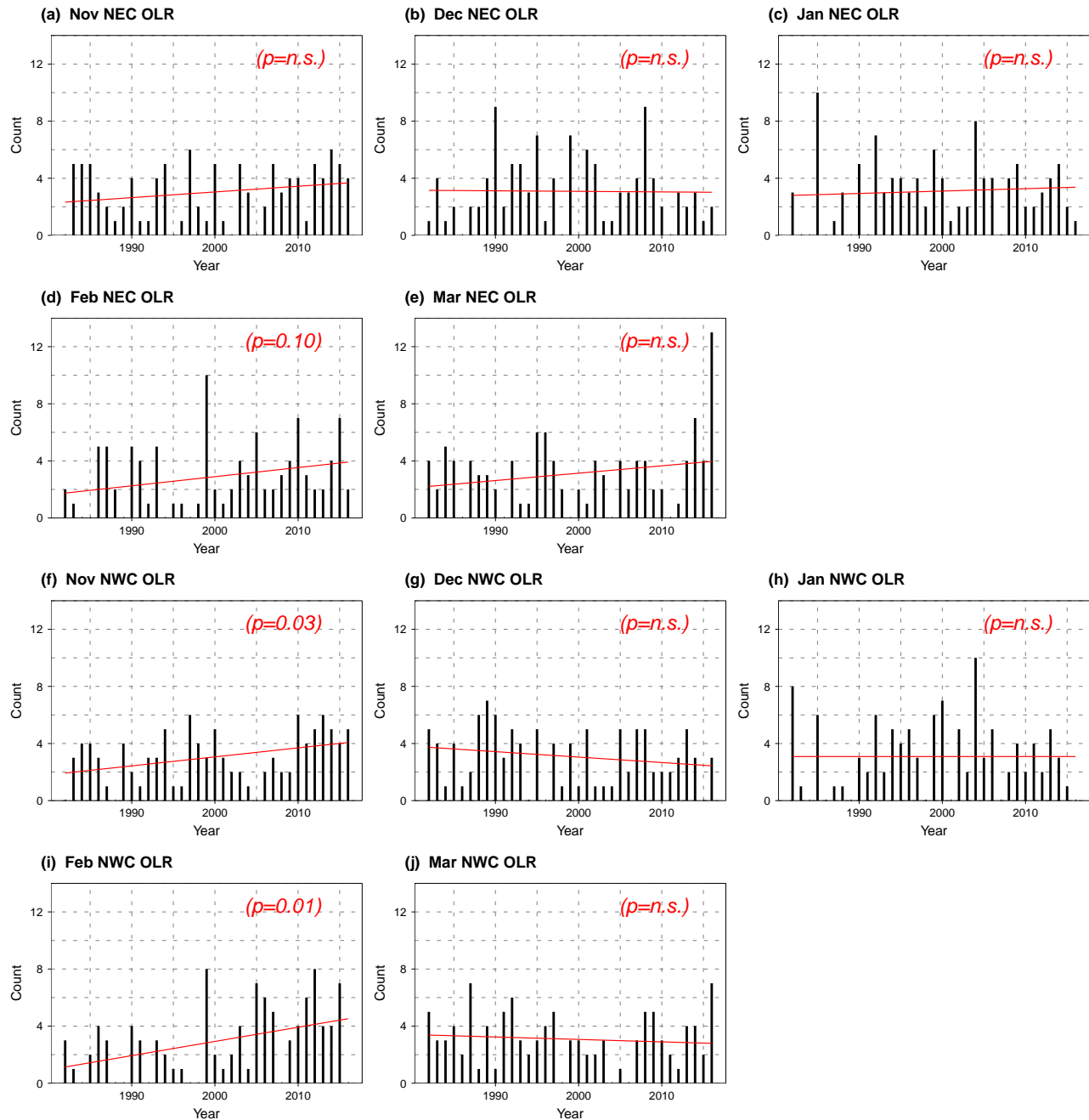


FIGURE S1

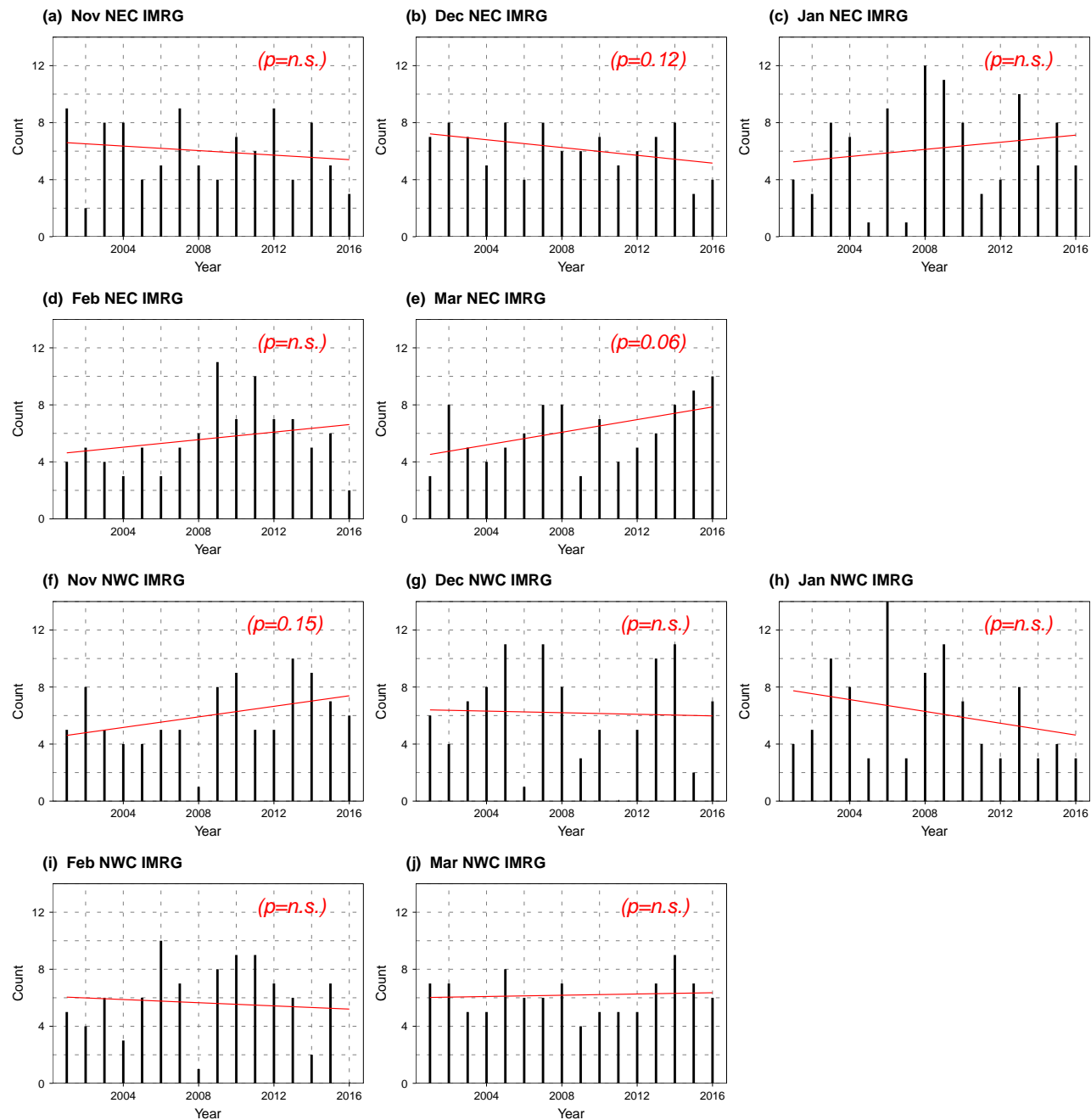


FIGURE S2

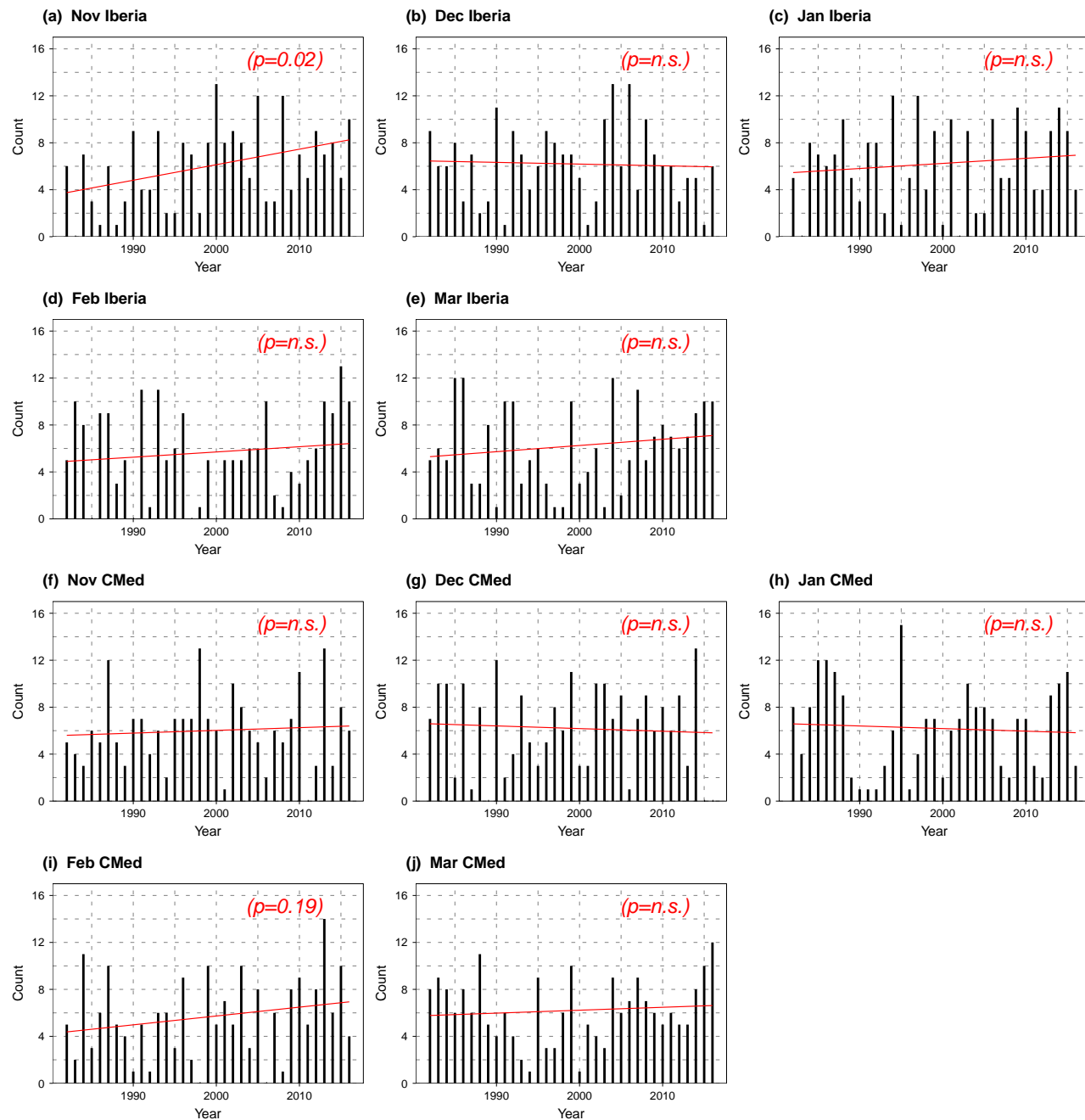


FIGURE S3

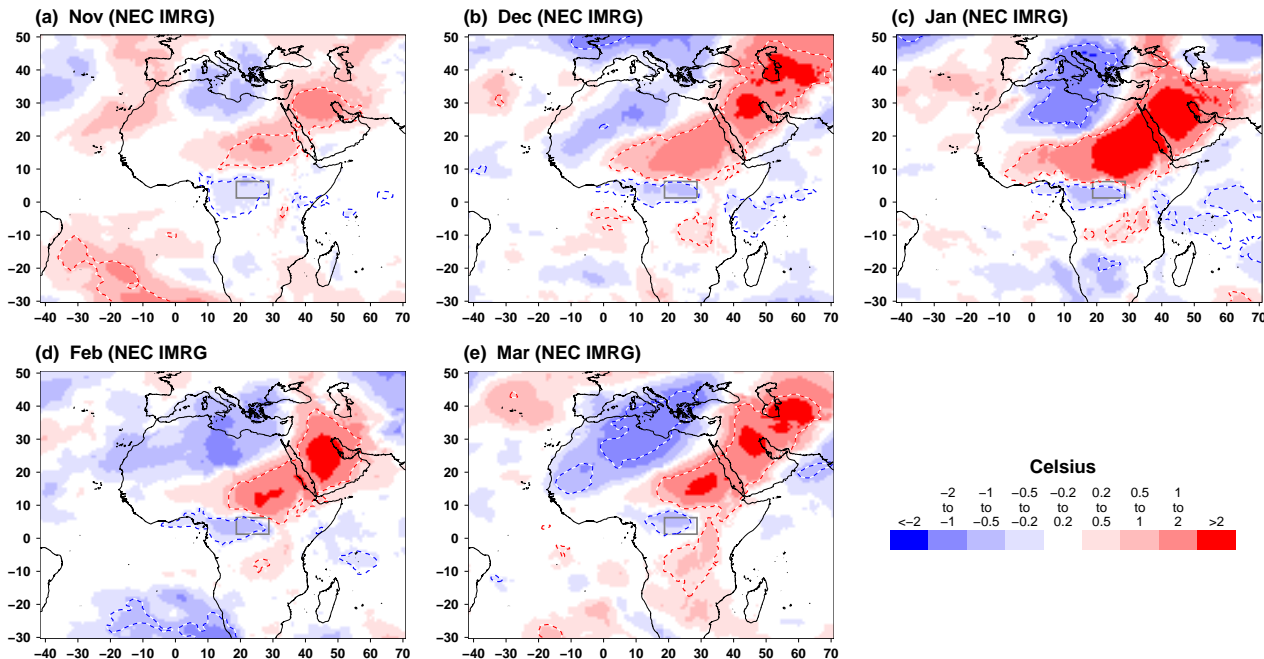


FIGURE S4

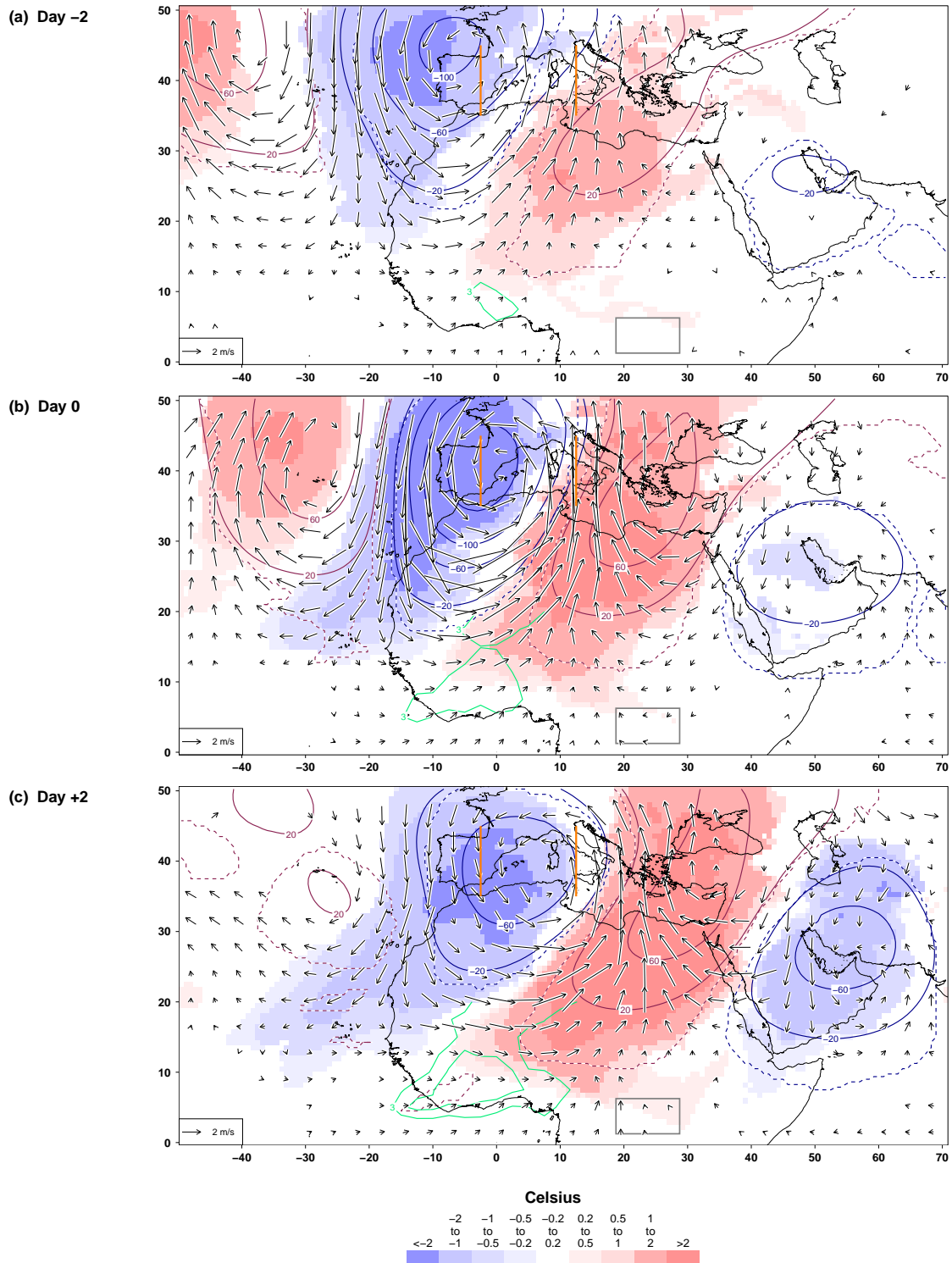


FIGURE S5

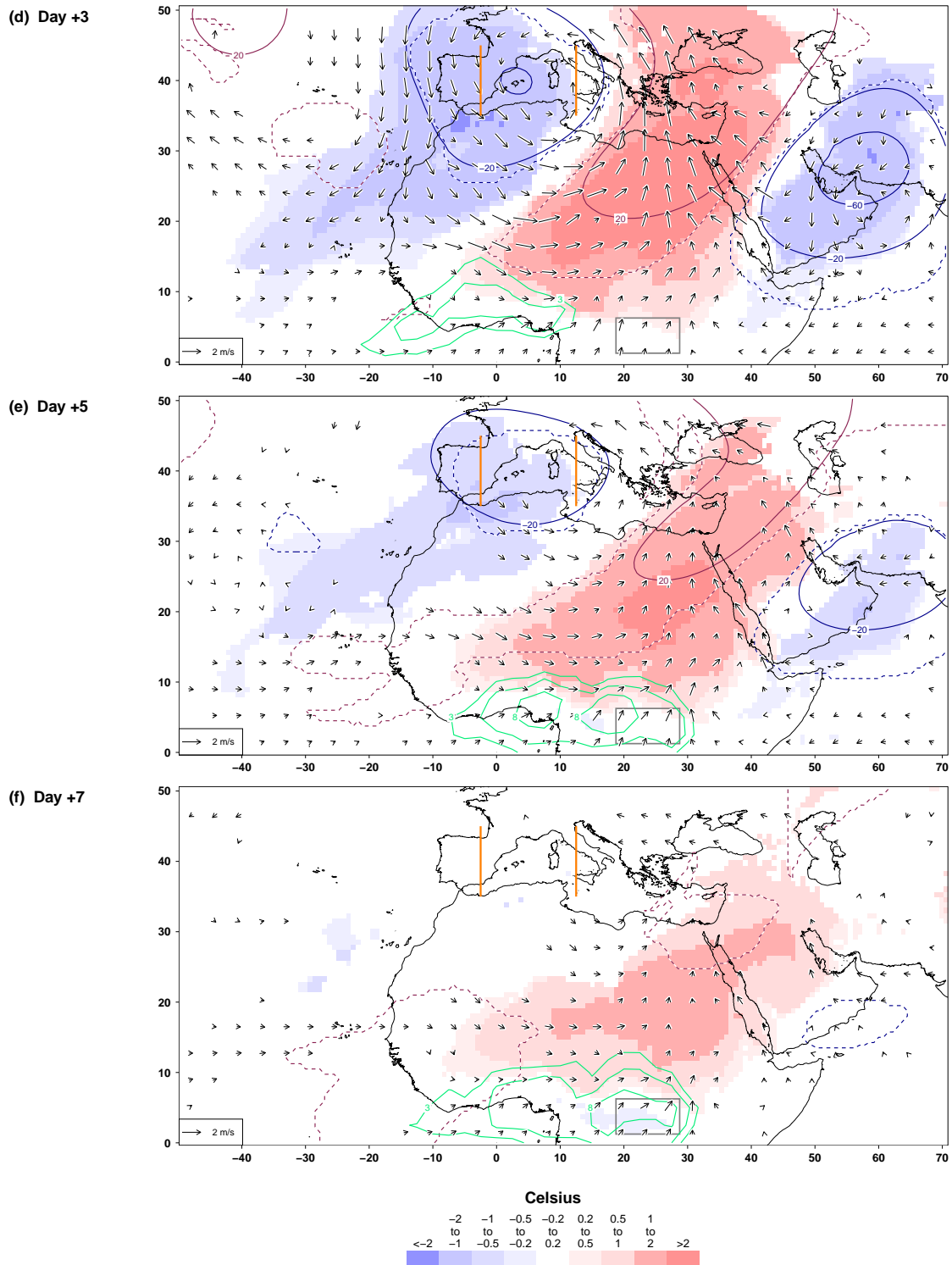


FIGURE S5 (continued)

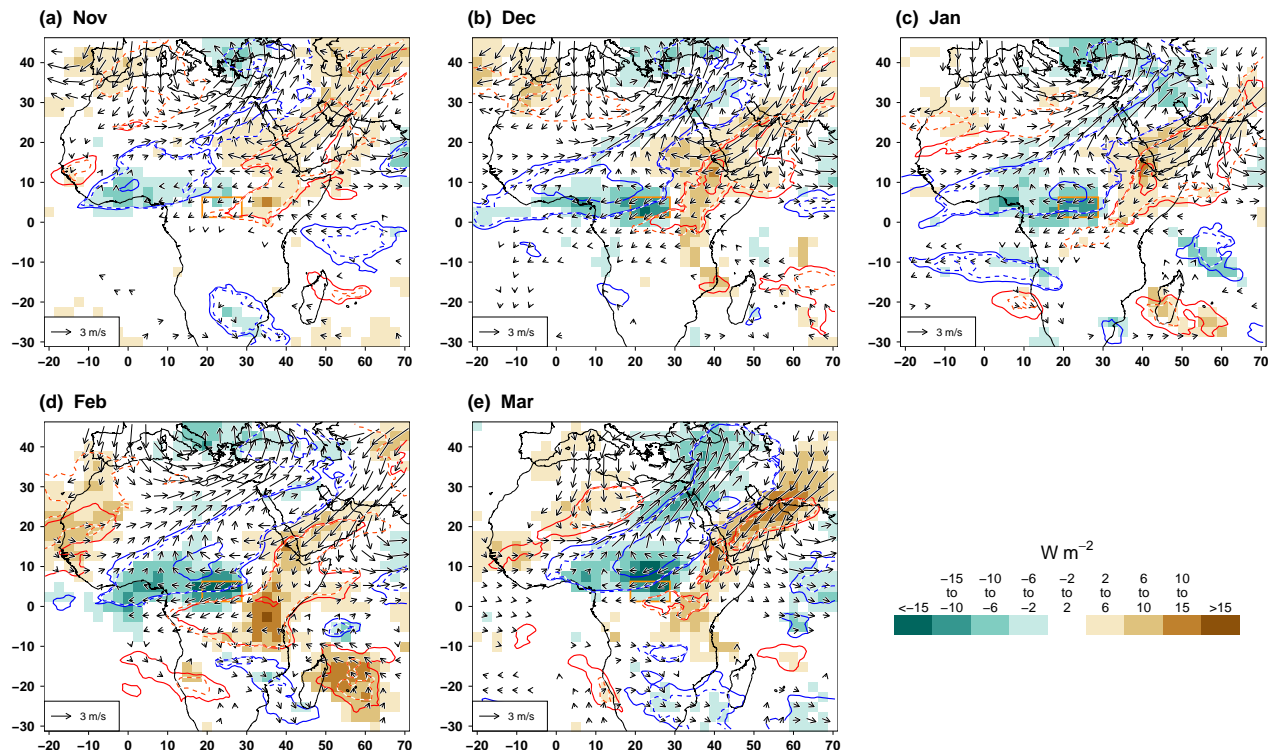


FIGURE S6

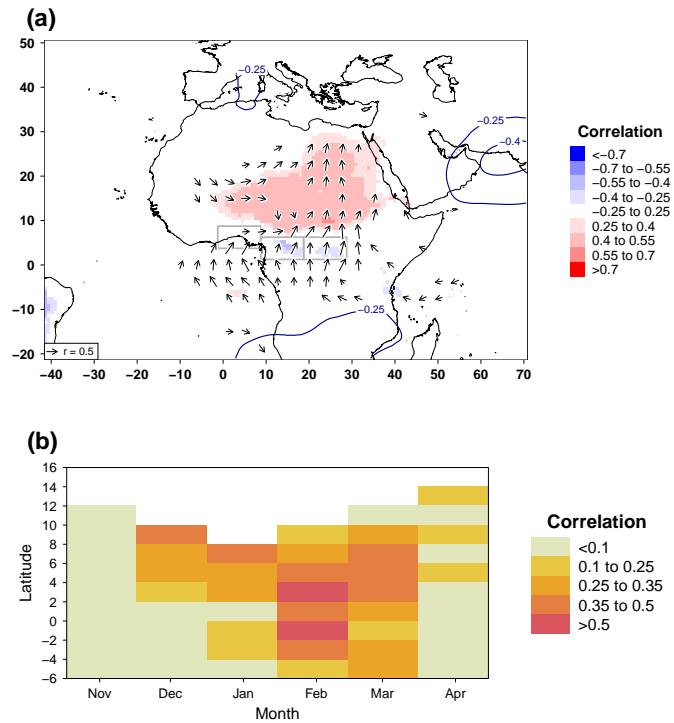


FIGURE S7